NANOSTRUCTURES BASED TERAHERTZ EMISSION

TAMANNA PUNIA

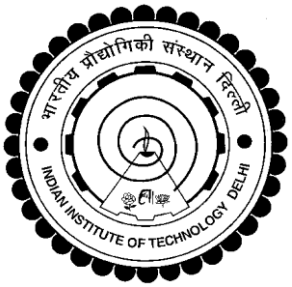

DEPARTMENT OF PHYSICS
INDIAN INSTITUTE OF TECHNOLOGY DELHI
OCTOBER 2022

NANOSTRUCTURES BASED TERAHERTZ EMISSION

by

TAMANNA PUNIA

Department of Physics

Submitted

in fulfillment of the requirements of the degree of Doctor of Philosophy

to the

INDIAN INSTITUTE OF TECHNOLOGY DELHI

OCTOBER 2022

Dedicated to

my family and loved ones

&

those

whoever inspired and encouraged me

Certificate

This is to certify that the thesis entitled "**Nanostructures based Terahertz Emission**" being submitted by **Ms. Tamanna Punia** is worthy of consideration for the award of the degree of Doctor of Philosophy and is a record of the original bonafide research work carried out by her under my guidance and supervision, and that the results contained in it have not been submitted in part or full to any other university or institute for award of any degree/diploma.

I certify that she has pursued the prescribed course of research. I approve the thesis for the award of the degree of Doctor of Philosophy.

Hitendra K. Malik

Professor

Department of Physics

Indian Institute of Technology Delhi

Acknowledgements

On completion of my Ph.D. thesis, I am grateful to the almighty God for giving me enough strength and patience throughout the journey to achieve this goal. The research work carried out in this thesis is due to the motivation and support of several people to whom I am immensely thankful.

Firstly, I would like to express my heartiest gratitude and profound appreciation to my Ph.D. thesis Supervisor, **Professor Hitendra K. Malik**, whose more than 30 years of research career and proficiency was priceless in developing the research problems which made my research experience more productive and joyful. How I met my supervisor, that is a story in itself!. He is the one, who has supported me in the worst phase of my doctoral degree. I feel privilege and lucky enough to get a 'guide' rather than just a thesis supervisor. His calm and delightful behaviour and positive attitude for his research work was the source of motivation for me even during hard times of my Ph.D. journey. His intelligent and skilled guidance had consistently encouraged me to improve my thinking and sharpen my skills which upgraded my work to another level. With utmost confidence and uprightness, I can say that my thesis supervisor was way more than just a guide. He was throughout the journey, is, would always be my advisor, my inspiration, my incubator and above all my shield! wherever I go in my life. The research work carried out in thesis would not have been feasible without his constant guidance and support. I am sure he is the best thesis advisor who understands and tries to bring the best skills in a particular student without giving unnecessary pressure on his students. His approach of guiding every student is different which makes the research work interesting for everyone. One can discuss any kind of problem whether professional or personal with him due to his friendly and supportive behaviour.

My sincere thanks are due to my SRC (Student Research Committee) members; **Prof. R.K. Varshney**, **Prof. Mayank Kumar** and **Prof. Amita Das** for their useful suggestions and reviews. I would like to thank **Prof. Ratnamala Chatterjee**, Head of the Physics Department, IIT Delhi, DRC Members and all the respected faculty members of Department of Physics, IIT Delhi.

My heartiest thanks to **Hon'ble Prof. K.P. Singh**, Vice-Chancellor, MJPR University Bareilly, UP and **Prof. Anushree Malik**, Center for Rural Development and Technology, IIT Delhi for understanding, guiding and giving me moral support, whenever required. I am extremely grateful to **Prof. R.K. Moudgil** and **Prof. Fakir Chand**, Physics Dept., KUK, **Prof. Manish K. Kashyap**, School of Physical Sciences, JNU, New Delhi (Ex faculty-KUK), **Prof. Ashish Aggarwal**, Physics Dept., GJUST, Hisar for their valuable suggestions and other faculty members of the Physics Dept., KUK. My warmest thanks to **Prof. Rashmi Rakshit** and **Prof. Abha Dev Habib** of Miranda House College, DU, **Sh. Raj Kumar Punia** (my uncle) and **Dr.**

Sunita Balayan (sister) and **teachers of my school** (K.L. Arya D.A.V Public School, Hisar) and all others who has helped me in forming me who I am today.

I would like to acknowledge the University Grant Commission (UGC), Government of India for granting the amount of Junior and Senior Research fellowships which helped me financially during the journey. I am grateful to all the members of Plasma Science and Technology (PST) Laboratory with a special thanks to seniors, **Dr. Dimple Tuteja** for her advices, discussions on the research topic and **Dr. Sheetal Punia** for learning MATLAB software. All other seniors and juniors also deserve thanks for their friendly and supportive behaviour. A kind thanks to my friends: Ms. Priyanka Yadav, Ms. Neha Garg, Ms. Kousalya V and Mr. Mohit Khosya of IIT Delhi and Ms. Rashmi, Mr. Raj Kumar always guided and pampered me with their caring nature during the journey.

Luckily, I have the privilege of having a family whose love and support helped me to get through every phase of my life and played a fundamental role in completion of my Ph.D. work,

My parents, **Dr. Kitab Singh Punia** and Smt. **Shakuntla Punia**, who raised me in a loving and growing environment to encourage me and be courageous in all the matters of life. They have always highlighted the importance of education and being independent in a girls' life. I cannot forget their sacrifices, guidance and breaking the norms of sending a small town child, specially a girl child to Delhi University for doing her graduation. It was their dream that pushed me towards higher education rather than doing a job. Everyone has a father, who deserves special attention, respect and care but my father is a gem. He is 'Everything to me!, My hero'. It's his confidence and trust in me which has helped me to transform into a strong, confident and independent person. His efforts and whatever he has done and doing for me is priceless which can never be repaid.

Sh. **Rajpal Pachaar** and Smt. **Kamlesh Pachaar**, my parent-in-laws, always treated me like their daughter and inspired me to stay in the campus hostel so that I can be more focussed and comfortable in doing my research work.

Mr. **Akshay Pachaar**, my husband taught me to stay calm, positive and progressive during my research work. His support, care and belief has always strengthened me during some weak moments of my journey. He is the one who says, "It will be the happiest day of my life when you (I) will complete my higher studies and become successful." His efforts are highly appreciated.

My elder brother Mr. **Sameer Poonia** always treated me like his daughter and supported me financially and emotionally in every possible way he can do. He is my strength, my shield and the moments we spent together during our childhood were immensely beautiful specially during the festival of Rakshabandhan.

My sister in-law Mrs. **Sonam Redhal** and cousin sister Ms. **Ritika** helped me in making correct choices in my life. Their best wishes always had special place in my heart.

Finally, my nephews Mr. **Reyansh Poonia** and Mr. **Prathwin Poonia** deserve a special thanks for understanding and providing a good environment at home for doing my work, whenever required.

Tamanna Punia

Abstract

THz radiation band (with wavelength 1 mm to 0.1 mm) separates the two high technology fields of science, i.e. photonics and electronics, and formulates an important region of electromagnetic spectrum. The remarkable appealing characteristics like non-invasive, low photon energy (non-ionizing) than the ionization energy of most of the biological molecules makes them useful in the medical imaging over perilous x-ray radiations. This riveting THz frequency range has phase sensitivity to polar compounds such as water and also lies around different molecular rotational and vibrational energies (e.g. water) that not only unwraps the useful enigmatic information about the chemical composition but also the chemical structure and internal dynamics of the samples, hence provides 'fingerprints' of various organic molecules and diagnosis of cancerous skin tissues by monitoring the changes in the water content (absorption in water) and cell density. Another lucrative feature of THz gap is the high quality of spatial resolution and penetration through non-polar polymers, dielectrics and packing materials that commences its contact free and uninterruptible applications in the detection of defects in the coating of tablets and tiles of space transportation system, inspection of products, security screening and recognizing concealed weapons and explosives. Therefore, the unique and volatile properties of this range makes the generation of these radiations a fascinating field for research.

The incoherent, broadband coherent and narrowband coherent are three types of THz radiations. Several experimental techniques and theoretical methods have been demonstrated for generating broadband coherent THz radiations which include photonic and electronics based sources. THz generation from nonlinear crystals via photoconductive antenna, optical rectification, laser-plasma interaction and laser-nanostructure interaction are photonic based sources. The mingling of two laser beams having different frequencies for molding an optical beat results in the continuous wave THz generation. The emitted radiations using laser-plasma interaction may not be frequency tunable, and presence of only few plasma parameters for modulating THz radiations is the downside for the aforesaid technique. Due to more number of controlling parameters in case of nanostructured materials, THz radiation generation via laser-nanostructure interaction is a prominent method to achieve frequency tunable and controllable THz radiations.

In the present thesis, a method is presented for the generation of THz radiation using laser-nanostructure interaction. The medium containing graphite nanoparticles (NPs) is employed as a nonlinear medium, and to make situation more realistic, various scattering mechanisms and restoring forces exerted by the electron clouds of the NPs have also been considered. Graphite NPs are chosen because their plasmon frequency lies in THz range and

because of its hexagonal crystal structure different orientations of basal planes is easy to realize. Precisely, the studies included in the thesis majorly revolves around generating multiple and multifocal THz radiations on account of their applications in the medical field. So, attempts have been made for generating high intensity THz radiations which are not only multifocal, convertible and controllable but also frequency tunable. For the fulfilment of the purpose, skew coshyperbolic Gaussian (SCGB) laser beam profile, which is itself bi-focal or uni-focal based on the value of its parameters and a medium having NPs in two different shapes, i.e. spherical and cylindrical, with two different orientations of the basal planes with respect to the direction of incident laser beam have been considered. The profile of SCGB beams are convertible to Gaussian or super-Gaussian profiles for specific values of laser beams' parameters. The amplitude and position of the emitted THz peaks are discussed due to the captivating profile of the laser beam. The role of orientation of basal planes with respect to the electric field of incident laser beam has been investigated. The shape of the NPs i.e. spherical (SNPs) and cylindrical (CNPs), inter-particle distance, aspect ratio has also been considered for achieving stronger THz radiations. The tuning of frequency can be realized such that two peaks are achieved due to the resonant excitation of the medium when beating frequency of lasers matches the plasmon frequency. In addition, multifocal THz emission is possible when an external static electric field is applied to the aforesaid medium. The mechanism of generation of different THz fields together with the comparative study between the fields (i.e. beating and induced field) has been performed. The role of external electrostatic field on emitted THz radiations has also been investigated. To check the role of nanostructure, the core-shell NPs are employed in the medium on account of finding changes in the emitted THz fields. For that, exhaustive studies have been performed on a medium having core-shell NPs in two different shapes along with the presence and absence of external electrostatic field. One advantageous feature of using core-shell NPs over solid simple NPs is that the emitted THz radiations can be tuned by changing the ratio of radius of core and shell. An interesting property of emitted THz radiations is that they are multifocal, convertible (bi-focal to uni-focal and vice-versa) and controllable. The present work is efficacious for the diagnosis and treating cancerous cells efficiently keeping in mind desired number of peaks and amplitude of emitted THz radiation. Not only this, the amount of injection for destroying only the infected cells of the human body can be regulated by controlling the flow of NPs by changing the core and shell radius.

सार

टेराहर्ट्ज़ (THz) विकिरण बैंड (तरंग दैर्ध्य 1 मिमी से 0.1 मिमी के साथ) विज्ञान के दो उच्च प्रौद्योगिकी क्षेत्रों, अर्थात् फोटोनिक्स और इलेक्ट्रॉनिक्स को अलग करता है, और विद्युत चुम्बकीय स्पेक्ट्रम का एक महत्वपूर्ण क्षेत्र तैयार करता है। अधिकांश जैविक अणुओं की आयनीकरण ऊर्जा की तुलना में गैर-आक्रामक, कम फोटॉन ऊर्जा (गैर-आयनीकरण) जैसी उल्लेखनीय आकर्षक विशेषताएं उन्हें खतरनाक एक्स-रे विकिरणों पर चिकित्सा इमेजिंग में उपयोगी बनाती हैं। इस रिवेटिंग THz फ़्रीक्वेंसी रेंज में पानी जैसे ध्रुवीय यौगिकों के लिए चरण संवेदनशीलता होती है और यह विभिन्न आणविक घूर्णी और कंपन ऊर्जा (जैसे पानी) के आसपास भी होती है जो न केवल रासायनिक संरचना के बारे में उपयोगी गूढ़ जानकारी को खोलती है बल्कि रासायनिक संरचना और आंतरिक गतिशीलता को भी उजागर करती है। नमूने, इसलिए विभिन्न कार्बनिक अणुओं के उंगलियों के निशान प्रदान करते हैं और पानी की सामग्री (पानी में अवशोषण) और सेल घनत्व में परिवर्तन की निगरानी करके कैंसरयुक्त त्वचा के ऊतकों का निदान करते हैं। THz गैप की एक और आकर्षक विशेषता गैर-ध्रुवीय पॉलिमर, डाइलेक्ट्रिक्स और पैकिंग सामग्री के माध्यम से स्थानिक रिज़ॉल्यूशन और पैठ की उच्च गुणवत्ता है जो अंतरिक्ष परिवहन प्रणाली की गोलियों और टाइलों की कोटिंग में दोषों का पता लगाने में इसके संपर्क मुक्त और अबाधित अनुप्रयोगों को शुरू करती है। उत्पादों का निरीक्षण, सुरक्षा जांच और छिपे हुए हथियारों और विस्फोटकों की पहचान करना। इसलिए, इस श्रेणी के अद्वितीय और अस्थिर गुण इन विकिरणों की पीढ़ी को अनुसंधान के लिए एक आकर्षक क्षेत्र बनाते हैं।

असंगत, ब्रॉडबैंड सुसंगत और संकीर्ण बैंड सुसंगत तीन प्रकार के THz विकिरण हैं। ब्रॉडबैंड सुसंगत THz विकिरण उत्पन्न करने के लिए कई प्रयोगात्मक तकनीकों और सैद्धांतिक तरीकों का प्रदर्शन किया गया है जिसमें फोटोनिक और इलेक्ट्रॉनिक्स आधारित स्रोत शामिल हैं। फोटोकॉन्डक्टिव एंटीना, ऑप्टिकल रेक्टिफिकेशन, लेज़र-प्लाज्मा इंटरेक्शन और लेज़र-नैनोस्ट्रक्चर इंटरैक्शन के माध्यम से नॉनलाइनियर क्रिस्टल से THz पीढ़ी फोटोनिक आधारित स्रोत हैं। एक ऑप्टिकल बीट को ढालने के लिए अलग-अलग आवृत्तियों वाले दो लेज़र बीमों के मिलन से निरंतर तरंग THz उत्पन्न होती है। लेज़र-प्लाज्मा इंटरैक्शन का उपयोग करने वाले उत्सर्जित विकिरण आवृत्ति ट्यून करने योग्य नहीं हो सकते हैं, और THz विकिरणों को संशोधित करने के लिए केवल कुछ प्लाज्मा पैरामीटर की उपस्थिति उपरोक्त तकनीक के लिए नकारात्मक पक्ष है। नैनोस्ट्रक्चर सामग्री के मामले में अधिक संख्या में नियंत्रित मापदंडों के कारण, लेज़र-नैनोस्ट्रक्चर इंटरैक्शन के माध्यम से THz विकिरण पीढ़ी आवृत्ति ट्यून करने योग्य और नियंत्रणीय THz विकिरण प्राप्त करने का एक प्रमुख तरीका है।

वर्तमान शोध ग्रंथ में, लेज़र -नैनोस्ट्रक्चर इंटरैक्शन का उपयोग करके THz विकिरण की पीढ़ी के लिए एक विधि प्रस्तुत की गई है। ग्रेफाइट नैनोकणों (एनपी) वाले माध्यम को एक गैर-रेखीय माध्यम के रूप में नियोजित किया जाता है, और स्थिति को और अधिक यथार्थवादी बनाने के लिए, विभिन्न बिखरने वाले तंत्र और एनपी के इलेक्ट्रॉन समूहों द्वारा लगाए गए बलों को बहाल करने पर भी विचार किया गया

है। ग्रेफाइट एनपी को इसलिए चुना जाता है क्योंकि उनकी प्लास्मोन आवृत्ति THz परास में होती है और इसकी हेक्सागोनल क्रिस्टल संरचना के कारण बेसल प्लेन के विभिन्न झुकावों को महसूस करना आसान होता है। संक्षेप में, शोध ग्रंथ में शामिल अध्ययन प्रमुख रूप से चिकित्सा क्षेत्र में उनके अनुप्रयोगों के कारण कई और बहुकेन्द्रीय THz विकिरण उत्पन्न करने के इर्द-गिर्द घूमते हैं । इसलिए, उच्च तीव्रता वाले THz विकिरण उत्पन्न करने के प्रयास किए गए हैं जो न केवल बहुकेन्द्रित, परिवर्तनीय और नियंत्रणीय हैं बल्कि आवृत्ति ट्यून करने योग्य भी हैं। उद्देश्य की पूर्ति के लिए, स्क्यू (तिरछा) कोशीपर्बिक गौसियन (एससीजीबी) लेज़र बीम रेखाचित्र, जो स्वयं अपने मापदंडों के मूल्य के आधार पर द्विनाभित या एक-नाभित है और एक माध्यम जिसमें दो अलग-अलग आकार में एनपी होते हैं, अर्थात् गोलाकार और बेलनाकार, के साथ घटना लेज़र बीम की दिशा के संबंध में बेसल प्लेन के दो अलग-अलग झुकावों पर विचार किया गया है। लेज़र बीम के मापदंडों के विशिष्ट मूल्यों के लिए एससीजीबी बीम की रेखाचित्र गौसियन या सुपर- गौसियन रेखाचित्र में परिवर्तनीय हैं। उत्सर्जित THz चोटियों के आयाम और स्थिति पर लेज़र बीम के मनोरम रेखाचित्र के कारण चर्चा की जाती है। घटना लेज़र बीम के विद्युत क्षेत्र के संबंध में बेसल प्लेनों के उन्मुखीकरण की भूमिका की जांच की गई है। एनपी के आकार अर्थात् गोलाकार (एसएनपीएस) और बेलनाकार (सीएनपी), अंतर-कण दूरी, पहलू अनुपात को भी मजबूत THz विकिरण प्राप्त करने के लिए माना गया है। आवृत्ति की ट्यूनिंग को इस तरह महसूस किया जा सकता है कि दो चोटियों को माध्यम के गुंजयमान उत्तेजना के कारण प्राप्त किया जाता है जब लेज़रों की धड़कन आवृत्ति प्लास्मोन आवृत्ति से मेल खाती है। इसके अलावा, बहुकेन्द्रीय THz उत्सर्जन संभव है जब एक बाहरी स्थैतिक विद्युत क्षेत्र को उपरोक्त माध्यम पर लागू किया जाता है। विभिन्न THz क्षेत्रों के निर्माण के तंत्र के साथ-साथ क्षेत्रों के बीच तुलनात्मक अध्ययन (अर्थात् बीटिगं और प्रेरित क्षेत्र) का प्रदर्शन किया गया है। उत्सर्जित THz विकिरणों पर बाहरी इलेक्ट्रोस्टैटिक क्षेत्र की भूमिका की भी जांच की गई है। नैनोस्ट्रक्चर की भूमिका की जांच करने के लिए, उत्सर्जित THz क्षेत्रों में परिवर्तन खोजने के कारण कोर-शेल एनपीएस को माध्यम में नियोजित किया जाता है। उसके लिए, बाहरी इलेक्ट्रोस्टैटिक क्षेत्र की उपस्थिति और अनुपस्थिति के साथ-साथ दो अलग-अलग आकृतियों में कोर-शेल एनपी वाले माध्यम पर विस्तृत अध्ययन किया गया है। ठोस सरल एनपी पर कोर-शेल नैनोकणों का उपयोग करने की एक लाभप्रद विशेषता यह है कि उत्सर्जित THz विकिरणों को कोर और शेल के त्रिज्या के अनुपात को बदलकर ट्यून किया जा सकता है। उत्सर्जित THz विकिरणों की एक दिलचस्प विशेषता यह है कि वे बहुकेन्द्रित, परिवर्तनीय (द्विनाभित से एक-नाभित और इसके विपरीत) और नियंत्रणीय हैं। वर्तमान कार्य कैंसर कोशिकाओं के निदान और उपचार के लिए प्रभावी रूप से चोटियों की वांछित संख्या और उत्सर्जित THz विकिरण के आयाम को ध्यान में रखते हुए प्रभावी है। इतना ही नहीं मानव शरीर की केवल संक्रमित कोशिकाओं को नष्ट करने के लिए इंजेक्शन की मात्रा कोर और शेल त्रिज्या को बदलकर एनपी के प्रवाह को अनुकूल करके नियंत्रित किया जा सकता है।

Table of Contents

List of Figures

Figure 2.7. Dependence of efficiency of THz radiation on the beam width and index of lasers in a medium having CNPs and SNPs equal in numbers with the parallel orientation of their basal planes, when $\left(\frac{n_{\alpha t_i}}{n_{0t_i}}\right) = 0.4$, y = 1.1b and s = 0.8.

Figure 2.8. Dependence of Efficiency of THz radiation on the geometry of NPs with the parallel orientation of their basal planes, when $\left(\frac{n_{\alpha t_i}}{n_{0t_i}}\right) = 0.4$, y = 1.1b and s = 0.8.

Figure 3.1. Solid thick line shows profile of a hat top beam, whereas the dotted line corresponds to the Gaussian beam.

Figure 3.2. Variation of ponderomotive force with transverse distance from the beam axis for different values of incident lasers electric field, when $\omega_1 = 1.884 \times 10^{14}$ rad/s, $\omega_2 = 1.811 \times 10^{14}$ rad/s, $h_c = 5r_c$ and $d_c = 6r_c$ of the nanocylinders.

Figure 3.3. Variation of emitted THz radiation field with normalized frequency for different inter-particle distance of the adjacent nanocylinders with their basal planes parallel to the incoming electric field, when $h_c = 5r_c$, $E_0 = 4.0 \times 10^{10}$ V/m, $b = 2.0 \times 10^{-5}$m and y = $0.95b$.

Figure 3.4. Spatial profile of emitted THz radiations with normalized distance from axis of beam for different values of height of nanocylinders with their basal planes parallel to the electric field of laser beams, when $d_c = 6r_c$, $E_0 = 4.0 \times 10^{10}$ V/m , $b = 2.0 \times 10^{-5}$m, $\omega_1 = 1.884 \times 10^{14}$ rad/s and $\omega_2 = 1.811 \times 10^{14}$ rad/s .

Figure 3.5. Variation of emitted THz radiation field with the beam width for different values of incident lasers field, when y = $0.95b$, $\omega_1 = 1.884 \times 10^{14}$ rad/s, $\omega_2 = 1.811 \times 10^{14}$ rad/s, $h_c = 5r_c$ and $d_c = 6r_c$ of the nanocylinders.

Figure 3.6. Dependence of efficiency on the normalized frequency for different values of beam width a_0 and ripple density, A = $\left(\frac{n_{\alpha,t_i}}{n_{0,t_i}}\right)$, when $d_c = 6r_c$, $h_c = 5r_c$, $E_0 = 4.0 \times 10^{10}$ V/m and y = $0.95b$. The medium contains only parallel oriented nanocylinders with respect to the electric field of the incident laser beam.

Figure 4.1. Variation of ponderomotive force with beam width for different combinations of coefficients of restoring force and damping constant when $E_0 = 6 \times 10^{10}\ V/m$, s = 1, p = 6, y = 0.85b, r_s= 100 nm, r_c = 50 nm, h_s= 300 nm, h_c = 150 nm, $d_{ss} = d_{cs} = 5r_s$ and $\omega = 1.25\ \omega_p$.

Figure 4.2. Variation of effective permittivity with radius of the core for different orientations of basal planes when $E_0 = 6 \times 10^{10}\ V/m$, s = 1, b = $2 \times 10^{-5} m$, p = 6, y = 0.85b, r_s= 100 nm, h_s= 300 nm, h_c = 150 nm, $d_{ss} = d_{cs} = 5r_s$ and $\omega = 1.25\ \omega_p$.

Figure 4.3. Variation of normalized THz field with normalized plasma frequency for different combinations of coefficient of restoring force and damping constant when $E_0 = 6 \times 10^{10}\ V/m$, s = 1, p = 6, b = $2 \times 10^{-5} m$, y = 0.85b, r_s = 100 nm, r_c = 50 nm, $d_{ss} = d_{cs} = 5r_s$, h_s= 300 nm and h_c = 150 nm.

Figure 4.4. Variation of normalized THz field with transverse distance from beam axis for different ratios of core to shell radius when $E_0 = 6 \times 10^{10}\ V/m$, s = 1, p = 6, b = $2 \times 10^{-5} m$, $\omega = 1.25\ \omega_p$, $d_{ss} = d_{cs} = 5r_s$, h_s= 300 nm and h_c = 150 nm.

Figure 4.5. Variation of normalized THz field with effective permittivity for different ratios of core to shell radius when $E_0 = 6 \times 10^{10}\ V/m$, s = 1, p = 6, b = $2 \times 10^{-5} m$, y = 0.85b, $\omega = 1.25\ \omega_p$, $d_{ss} = d_{cs} = 5r_s$, h_s= 300 nm and h_c = 150 nm.

Figure 4.6. Variation of normalized THz field with radius of the core for different values of shell radius when $E_0 = 6 \times 10^{10}\ V/m$, s = 1, b = $2 \times 10^{-5} m$, p = 6, y = 0.85b, $d_{ss} = d_{cs} = 5r_s$, h_s= 300 nm and $\omega = 1.25\ \omega_p$.

Figure 4.7. Distribution of efficiency with beam width for different values of the ratio of inter-particle distance between shells of the NPs and radius of the shell when $E_0 = 6 \times 10^{10}\ V/m$, s = 1, p = 6, y = 0.85b, h_s= 300 nm, h_c = 150 nm and $\omega = 1.25\ \omega_p$.

Figure 5.1. Schematic of excitation of THz radiation in presence of external periodic electric field via interaction between laser and medium containing spherical and cylindrical NPs.

Figure 5.2. Behavior of beating and induced force with transverse distance from beam axis, when $n_{\alpha t_i} = 0.45 n_{0t_i}$, b = 1×10^{-5} m, s = 0.5, $\omega = 1.25\omega_p$, $d_{sti} = d_{cti} = 6r_{sti}$, $h_{cti} = 4\ r_{cti}$ and p = 6.

Figure 5.3. Dependence of the induced ponderomotive force with transverse distance from the beam axis for different values of laser index and skewness parameter, when $n_{\alpha t_i} = 0.45 n_{0t_i}$, $\omega = 1.25\omega_p$, $d_{sti} = d_{cti} = 6r_{sti}$, $h_{cti} = 4\ r_{cti}$ and b = 1×10^{-5} m.

Figure 5.4. Behavior of induced ponderomotive force with transverse distance from beam axis with either parallel or perpendicular orientations of basal planes with respect to the electric field of the incident laser beam, when $n_{\alpha t_i} = 0.45 n_{0t_i}$, s = 0.5, p = 6, $\omega = 1.25\omega_p$, $d_{sti} = d_{cti} = 6r_{sti}$, $h_{cti} = 4\ r_{cti}$ and b = 1×10^{-5} m.

Figure 5.5. Distribution of beating and induced field with transverse distance from beam axis for parallel orientation of the basal planes of the NPs, when $n_{\alpha t_i} = 0.45 n_{0t_i}$, b = 1×10^{-5} m, s = 0.5, $\omega = 1.25\omega_p$, $d_{sti} = d_{cti} = 6r_{sti}$, $h_{cti} = 4\ r_{cti}$ and p = 6.

Figure 5.6. Variation of beating and induced field with normalized frequency for only parallel orientation of the basal planes, when $n_{\alpha t_i} = 0.45 n_{0t_i}$, b = 1×10^{-5} m, s = 0.5, y = 0.8b, $d_{sti} = d_{cti} = 6r_{sti}$, $h_{cti} = 4\ r_{cti}$ and p = 6.

Figure 5.7. Variation of induced field with transverse distance from beam axis for different orders of incident laser beam when $n_{\alpha t_i} = 0.45 n_{0t_i}$, b = 1 × 10^{-5} m, s = 0.5, $d_{sti} = d_{cti} = 6r_{sti}$, $h_{cti} = 4\ r_{cti}$ and p = 6.

Figure 5.8. Variation of induced field with normalized frequency for parallel orientation of the basal planes with respect to the electric field of the incident laser beam when $n_{\alpha t_i} = 0.45 n_{0t_i}$, b = 1 × 10^{-5} m, s = 0.5, y = 0.8b, $d_{sti} = d_{cti} = 6r_{sti}$, $h_{cti} = 4\ r_{cti}$ and p = 6.

Figure 5.9. Variation of induced field with beam width for different values of ripples in the density and magnitude of external electric field when s = 0.5, y = 0.8b, $\omega = 1.25\omega_p$, $d_{sti} = d_{cti} = 6r_{sti}$, $h_{cti} = 4\ r_{cti}$ and p = 6.

Figure 5.10. Distribution of induced efficiency for different heights of cylindrical NPs and inter-particle distances between NPs, when $n_{\alpha t_i} = 0.45 n_{0t_i}$, b = 1 × 10^{-5} m, s = 0.5, y = 0.8b, $\omega = 1.25\omega_p$, $d_{sti} = d_{cti} = 6r_{sti}$, $h_{cti} = 4\ r_{cti}$ and p = 6.

Figure 6.1. Distribution of beating and induced force with transverse distance from beam axis, when $E_0 = 6 \times 10^{10}\ V/m$, $E_{0p} = 4 \times 10^{6}\ V/m$, s = 1, p = 6, $n_{\alpha t_i} = 0.45 n_{0t_i}$, b = 2 × $10^{-5} m$, r_s= 100 nm, r_c = 50 nm, h_s= 300 nm, h_c = 150 nm, $d_{ss} = d_{cs} = 5r_s$ and $\omega = 1.25\ \omega_p$.

Figure 6.2. Variation of beating and induced force with beam width when, $E_0 = 6 \times 10^{10}\ V/m$, $E_{0p} = 4 \times 10^{6}\ V/m$, s = 1, p = 6, $n_{\alpha t_i} = 0.45 n_{0t_i}$, y = 0.9b , r_s= 100 nm, r_c = 50 nm, h_s= 300 nm, h_c = 150 nm, $d_{ss} = d_{cs} = 5r_s$ and $\omega = 1.25\ \omega_p$.

Figure 6.3. Distribution of beating THz field with normalized plasma frequency for different ratios of aspect ratios of core, when $E_0 = 6 \times 10^{10}\ V/m$, $E_{0p} = 4 \times 10^{6}\ V/m$, s = 1, p = 6, b = 2 × $10^{-5} m$, y = 0.9b, r_s = 100 nm, $d_{ss} = d_{cs} = 5r_s$, h_s= 300 nm.

Figure 6.4. Variation of beating and induced THz field with normalized plasma frequency when $E_0 = 6 \times 10^{10}\ V/m$, $E_{0p} = 4 \times 10^{6}\ V/m$, s = 1, p = 6, b = 2 × $10^{-5} m$, y = 0.9b, r_s = 100 nm, r_c = 50 nm, $d_{ss} = d_{cs} = 5r_s$, h_s= 300 nm and h_c= 150 nm.

Figure 6.5. Distribution of induced THz field with external electric field when $E_0 = 6 \times 10^{10}\ V/m$, s = 1, $\omega = 1.25\ \omega_p$, p = 6, b = 2 × $10^{-5} m$, y = 0.9b , $d_{ss} = d_{cs} = 5r_s$, h_s= 300 nm and h_c= 150 nm.

Figure 6.6. Distribution of II peak (transverse resonance peak) of induced THz field with inter-particle distance between NPs when $E_0 = 6 \times 10^{10}\ V/m$, $E_{0p} = 4 \times 10^{6}\ V/m$, s = 1, $\omega = 1.25\ \omega_p$, p = 6, b = 2 × $10^{-5} m$, y = 0.9b, h_s= 300 nm and h_c= 150 nm.

Figure 6.7. Behavior of induced efficiency with external electric field for different values of laser index when, $E_0 = 6 \times 10^{10}\ V/m$, s = 1, y = 0.9b, r_s = 100 nm, r_c = 50 nm, h_s= 300 nm, h_c = 150 nm and $\omega = 1.25\ \omega_p$.

List of Symbols

α ……Wave number of density ripples
α_c……Restoring force coefficient for CNPs

α_s……Restoring force coefficient for SNPs

i……...Denotes configuration of basal planes

$\overrightarrow{E_J}$…….Electric field of skew-coshyperbolic Gaussian laser beam

$\vec{E}_p$……....Electric field of external electrostatic field

$\vec{E}_{THz}$……....Electric field of emitted THz radiation (Chapters-2,3 and 4)
E_0……Peak amplitude of Laser Electric field

E_{0p}…….....Peak amplitude of external electrostatic field

$\vec{E}_{0THz1}$…….Beating field (Chapters-5 and 6)
$\vec{E}_{0ITHz2}$……....Induced field 1(Chapters- 5 and 6)
$\vec{E}_{0ITHz3}$……....Induced field 2 (Chapters- 5 and 6)
$\varepsilon(c)$…….Permittivity of cylindrical NPs
$\varepsilon(s)$…….Permittivity of spherical NPs
ε_c…….Permittivity of the core
ε_{eff}…….Effective permittivity of the medium
ε_h……Permittivity of host medium
ε_s……Permittivity of the shell
$\varepsilon_c(cs)$…….Permittivity of cylindrical core-shell NPs
$\varepsilon_s(cs)$…….Permittivity of spherical core-shell NPs
ε^{free}……...Permittivity of free electrons
ε_{t_i}……...Permittivity of bound electrons in particular orientation of basal planes
ε_i^{bound}…….....Permittivity of bound electrons
η…….Efficiency of the scheme
$\eta_{Induced}$…….Efficiency due to induced field
A…….Ratio of density ripples and the density of the conduction electrons
$\vec{X}^{NL}$…….Position vector of electron cloud due to ponderomotive force
ω…….Beating frequency of the lasers
ω_j……Angular Frequencies of first and second incident laser

ω_p……...Plasma frequency of electrons

$\omega_{p_{t_i}}$……Plasma frequency of electrons in particular orientation

k……..Beating wavenumber of the lasers
k_j…….Propagation vector of laser 1 and 2
k_1'……..Modified wavenumber of beating field
k_2'……Modified wavenumber of induced field 1
k_3'……Modified wavenumber of induced field 2
Q…….....Symbol defined in the respective chapters
γ_c……Damping constant for cylindrical shell
γ_s……Damping constant for spherical shell
γ_{0p}…….....Periodicity of external electrostatic field
Γ_b……Damping due to surface scattering of conduction electrons in the shell of NPs
Γ_d……Bulk damping coefficient
$\Gamma_{d\perp,\parallel}$……Bulk damping coefficient in particular orientation of basal planes
Γ_{e-e}…….Damping due to scattering of an electron by another one in a bulk lattice of metal
Γ_{e-ph}……...Damping due to interaction of conduction electrons with metallic lattice
Γ_{rad}…….Damping due to radiation of accelerated electrons
Γ_{surf}……....Damping due to scattering of surface electrons
j……...Denotes two kinds of lasers (laser 1 and 2)
$\vec{J}^{NL}$.....Nonlinear current density
J_{PY1}^{NL}…….....Nonlinear current density due to beating of lasers (Chapters- 5 and 6)
J_{IPY2}^{NL}……Nonlinear current density due to coupling of laser 1 with external field
J_{IPY3}^{NL}……Nonlinear current density due to coupling of laser 2 with external field
t_i…….Symmetry axis normal to the plane inside a nanoparticle
$< W_L >$……...Average energy density of incident laser
$< W_{THz} >$…...Average energy density of the emitted THz field
d_{cs}…….Inter-particle distance between two cylindrical shells (Chapters- 4 and 6)
d_{ss}……...Inter-particle distance between two spherical shells (Chapters- 4 and 6)
d_{ct_i}…….....Inter-particle distances between any two CNPs in a particular orientation
d_{st_i}…….....Inter-particle distances between any two SNPs in a particular orientation
n…….....Order of the laser beam
n_α……...Density ripples in the medium
n_{oc}……..Macroscopic density of CNPs
n_{os}……..Macroscopic density of SNPs

n_0……...Total macroscopic density of the NPs

n_{0t_i}…….Total density of the NPs in a particular orientation of basal planes

n'……....Modulation in the macroscopic density of each kind of NP
p……..Lasers' index

P…….Symbol defined in the corresponding chapters
f_c…….Volume fractions of the core (Chapters- 4 and 6)
f_s…….Volume fractions of the shell (Chapters- 4 and 6)
f_{ct_i}……...Volume fraction of CNPs in a particular orientation (Chapters- 2,3 and 5)

f_{st_i}……...Volume fraction of SNPs in a particular orientation (Chapters- 2 and 5)

ϕ_p……Ponderomotive potential

$\vec{F}_P^{NL}$…….....Nonlinear ponderomotive force
$\vec{F}_{Py}^{NL}$……..Y-component of nonlinear ponderomotive force
F_{PY1}^{NL}……Ponderomotive force due to beating of lasers (Chapters- 5 and 6)

F_{IPY2}^{NL}…….....Ponderomotive force due to coupling of laser 1 with external field
F_{IPY3}^{NL}…….....Ponderomotive force due to coupling of laser 2 with external field
$\vec{F}_{Pz}^{NL}$……...Z-component of nonlinear ponderomotive force
b……Beam width of the laser beam

β_c……..Permittivity constant for CNPs
β_s……..Permittivity constant for SNPs
r_c…….....Average radii of core (Chapters- 4 and 6)
$\vec{r_j}$……...Position vector of the electron cloud due to laser 1 and 2

r_s…….....Average radii of shell (Chapters- 4 and 6)
r_{cc}…….Average radii of cylindrical core (Chapters- 4 and 6)
r_{cs}…….Average radii of cylindrical shell (Chapter- 4 and 6)
r_{sc}…….Average radii of spherical core (Chapters- 4 and 6)
r_{ss}…….Average radii of spherical shell (Chapters- 4 and 6)
r_{ct_i}……...Average radii of CNPs (Chapters- 2,3 and 5)
r_{st_i}……...Average radii of SNPs (Chapters- 2,3 and 5)
R……..Symbol defined in the respective chapters
λ_b……Mean free path of electrons in the shell
$\vec{v}_f$……Fermi velocity of the electrons
$\overrightarrow{v_j}$…….....Oscillatory velocity of electron clouds due to laser 1 and 2
$\vec{v}^{NL}$…….....Nonlinear velocity of the electron cloud
v_y^{NL}……..Y-component of nonlinear velocity
V……..Volume of the thickness of the shell
s……...Skewness parameter of the laser beam

S…….Surface area of the shell of the NPs
h_c……...Height of the core (Chapters- 4 and 6)
h_s……...Height of the shell (Chapters- 4 and 6)
h_{ct_i}…….Height of the CNPs in a particular orientation (Chapters- 2,3 and 5)

List of Abbreviations

1D	One-Dimensional
2D	Two-Dimensional
3D	Three-Dimensional
BCS	Bardeen-Cooper-Schrieffer Theory
BCWC	Body-Centric Wireless Communication
BWO	Backward-Wave Oscillators
CNPs	Cylindrical Nanoparticles
CPA	Chirped-Pulse Amplification
CVD	Chemical Vapor Deposition
CW	Continuous Wave
DNA	Deoxyribonucleic Acid
EM	Electromagnetic
EMR	Electromagnetic Radiations
ES	Electrostatic Field
FDTD	Finite-Difference Time-Domain
FEL	Free Electron Laser
IMPATT	Impact Ionization Avalanche Transit-Time Diode
ISO	International Organization for Standardization
LAN	Local Area Network
MATLAB	Matrix Laboratory
NDT	Non-Destructive Technique
NPs	Nanoparticles
NRs	Nanorods
PCA	Photoconductive Antenna
PM	Particulate Matter
QD	Quantum-Dot
SCGB	Skew Coshyperbolic Gaussian beam
SNPs	Spherical Nanoparticles
TCI	Terahertz Chemical Imaging
THz	Terahertz
THz-TDS	Terahertz Time- Domain Spectroscopy
TWT	Travelling-Wave Tube
UGC	University Grant Commission
US-FCC	United States-Federal Communications Commission
VED	Vacuum Electronic Devices